8 Supplementary Material

In the following we provide a semi-quantitative model description of the experimental requirements for phase resolved imaging of E_z using weak-field homodyne interferometric amplification. Without loss of generality, we choose a simple model behavior for the distance dependence of the E_z field component of the plasmonic nanostructure at a fixed location above its surface as $E_z = E_0 \exp[\frac{-z}{d_0}]$ with decay length d_0. The motion of the AFM tip as a scattering probe is described by a harmonic function $z(t) = d+a[1+\cos(\omega_d t)]$ oscillating around an average height $d + a$ above the surface with amplitude a and distance of closest approach d as shown schematically in Fig 5.

The total signal at the detector has two sources, the near-field scattered by the tip $\propto E_z$ and the reference field from the interferometer $E_{\text{ref}} \exp[i(\omega t + \Phi_{\text{ref}})]$ of adjustable amplitude E_{ref} and phase Φ_{ref}. In the limit that the amplitude of cantilever oscillation a is smaller than the exponential decay constant d_0, i.e., $a < d_0$, the total field can be approximated by a series expansion:

$$\begin{aligned} E_{\text{out}}(z,t) &= E_{\text{ref}} \exp[i(\omega t + \Phi_{\text{ref}})] \\ &\quad + E_0 \exp[\frac{-z}{d_0}] \exp[i(\omega t + \Phi_{\text{nf}})] \qquad (2) \\ &\approx E_{\text{ref}} \exp[i(\omega t + \Phi_{\text{ref}})] \\ &\quad + E_0(1 - \frac{z}{d_0} + \frac{z^2}{2d_0^2}) \exp[i(\omega t + \Phi_{\text{nf}})], \qquad (3) \end{aligned}$$

with Φ_{nf} and Φ_{ref} representing the optical phases of the near-field signal and reference field, respectively. Equation 3 can be expressed as a Fourier series in terms of harmonics of the cantilever oscillation as

$$\begin{aligned} E_{\text{out}}(t) &= E_{\text{ref}} \exp[i(\omega t + \Phi_{\text{ref}})] \\ &\quad + \sum_{n=0}^{2} A_n \cos[n\omega_d t] \exp[i(\omega t + \Phi_{\text{nf}})], \qquad (4) \end{aligned}$$

with the coefficients A_n given by:

$$A_0 = E_0\left(1 - \frac{a+d}{d_0} + \frac{2d^2+4ad+3a^2}{4d_0^2}\right) \quad (5)$$

$$A_1 = E_0\left(-\frac{a}{d_0} + \frac{a(a+d)}{d_0^2}\right) \quad (6)$$

$$A_2 = E_0\left(\frac{a^2}{4d_0^2}\right). \quad (7)$$

Hence, the detected intensity, $I_{\text{out}}(t) = E_{\text{out}}(t)\cdot E^*_{\text{out}}(t)$, expressed in terms of harmonics of ω_d is

$$I_{\text{out}}(t) = \sum_{n=0}^{4} I_n \cos[n\omega_d t]. \quad (8)$$

The magnitudes of the first and second harmonic terms, which are typically measured in s-SNOM, are given by

$$|I_1| = |2E_{\text{ref}}A_1\cos[\Phi] + 2A_0A_1 + A_1A_2|, \text{ and} \quad (9)$$

$$|I_2| = |2E_{\text{ref}}A_2\cos[\Phi] + 2A_0A_2 + A_1^2/2|, \quad (10)$$

with $\Phi = \Phi_{\text{ref}} - \Phi_{\text{nf}}$ representing the phase difference between the reference and tip scattered fields.

Fig. 6(a) displays the expected dependence of $|I_2|$ on Φ for different reference field amplitudes E_{ref}. Corresponding experimental results acquired over the end of a Ag wire under p polarized optical excitation are shown in Fig. 6(b) for reference amplitudes corresponding to the regimes where $E_{\text{ref}} \gg E_0$, $E_{\text{ref}} \approx E_0$, and $E_{\text{ref}} < E_0$. The excellent agreement confirms the applicability of the assumptions made.

For most practical applications, two interferometric homodyne amplification regimes can be distinguished: the conventional strong amplification with $E_{\text{ref}} \gg E_0$, and the weak amplification applied here with $E_{\text{ref}} \sim E_0$. For $E_{\text{ref}} \gg E_0$, the first term in Eqns. 9 and 10 becomes dominant which results in strong amplification of the scattered near field when the reference signal is either in or out of phase with the scattered near-field as shown. Signal intensity minima exist when the first term vanishes for $\Phi = \pi/2$. This behavior is seen in Fig. 6(a) (solid line) showing a simulation of the second-harmonic signal using Eqn. 10 in comparison with corresponding experimental results (b).

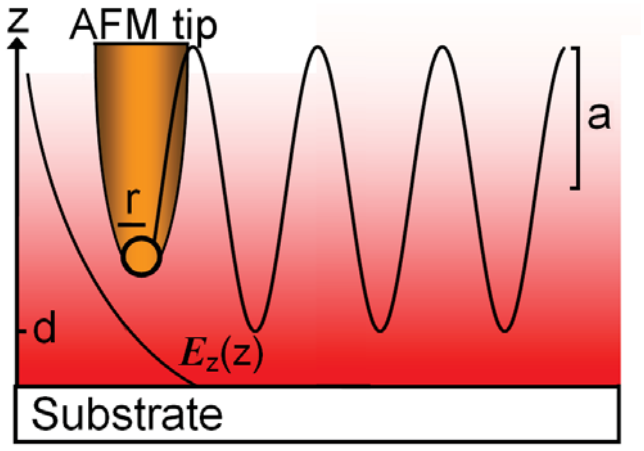

Figure 5: Model of the experimental configuration for the simulated detected near-field under weak homodyne amplification.

As the amplitude of the reference field is decreased, in addition to an expected decrease in the detected signal at the cantilever harmonic frequencies, the phases in which constructive and destructive interference occur also change. For a given cantilever harmonic, as the strength of the reference field is decreased from the strong amplification limit, the cusp shaped minima originally located at $\Phi = \pi/2$ and $\Phi = 3\pi/2$ begin to approach one another eventually merging to form a single minimum at $\Phi = \pi$ when $E_{\rm ref} \simeq E_0$. This is characteristic of a weak homodyne amplification regime in which constructive and destructive interference occurs for phases of $\Phi = 0$ and $\Phi = \pi$, respectively. The transition from the strong, to intermediate, and finally to the weak-homodyne amplification regime is illustrated in Fig. 6 by the solid, dashed, and dotted lines, respectively.

It should be noted that this model does not include the far-field background scattering self-homodyne field $E_{\rm bg}$ as an additional contribution. This background electric field is present due to far-field back scattering from the sample roughness and the tip shaft. It is characterized by a relative phase dependence on the spatial distribution of scattering centers resulting in a self-homodyne amplification of the near-field signal from the tip. This signal is observed in our measurements giving rise to a constant signal offset.

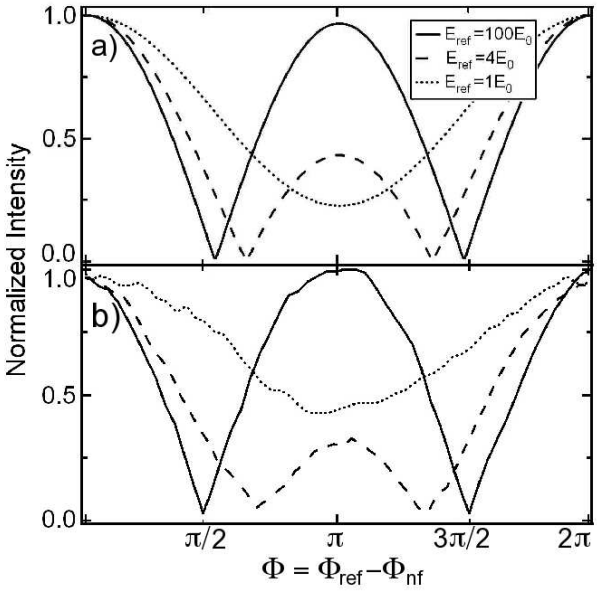

Figure 6: Simulated (a) and experimental (b) *s*-SNOM signal intensity variations as a function of the phase difference between near-field and reference phase $\Phi = \Phi_{\mathrm{ref}} - \Phi_{\mathrm{nf}}$ for three different ratios of near-field and reference field amplitudes E_{ref}/E_0 of 100 (solid line), 4 (dashed line), and 1 (dotted line). The weak homodyne case (dotted) with minima and maxima at respective out-of-phase near-field regions, thus provides direct visualization of mode behavior.